Pergamon

Journal of Structural Geology, Vol. 19, No. 10, pp. 1343 to 1358, 1997

0191-8141/97 $17.00 + 0.00

PII: S0191-8141(97)00044-8

Exhumation of high-pressure granulites and the role of lower crustal advection in the North China Craton near Datong

P. H. G. M. DIRKS

Department of Geology, University of Zimbabwe, P.O. Box MP 167, Harare, Zimbabwe

J. S. ZHANG

Institute of Geology, State Seismological Bureau, P.O. Box 634, 100029 Beijing, China

and

C. W. PASSCHIER

Department of Geology, University of Mainz, 55099 Mainz, Germany

(*Received* 24 *October* 1996; *accepted in revised form* 19 *May* 1997)

Abstract—Granulites in the Datong-Huai'an area of North China are characterized by high *P–T* assemblages (14–16 kbar, ~900°C) that underwent decompression cooling to ~7 kbar and ~800°C during a 2500–2400 Ma tectonic event. Nearly all structures in the grantilites developed during the retrograde exhumation history, and can be subdivided into: (1) the stratigraphically lower, 'lower structural domain' that is characterized by complex folding with 55–10 km wide domes surrounded by concentric troughs, preserving concentric lineation patterns; and (2) the stratigraphically higher 'upper structural domain' that is characterized by a planar gneissic foliation, upright folds and a constant, shallowly SW-plunging, lineation pattern. During exhumation rocks probably passed from the 'lower' into the 'upper structural domain'.

Domes, recumbent folds and transposition fabrics resulted from a dynamic interplay between vertical (advective) flow and horizontal flattening. The 'lower structural domain' preserves structures reflecting the dominance of vertical flow while the 'upper structural domain' preserves structures that resulted from flattening and lateral flow. Horizontal flattening and lateral flow of domal structures led to total destruction of the domal geometries by transposition in a younger, horizontal gneissic layering. The process of doming, flattening and transposition repeated itself as advective exhumation of the high-pressure rocks progressed. Horizontal fabrics appear the more stable geometry and domes progressively degenerated into horizontal lensoidal shapes, probably as a result of the low viscosities of the granulites.

Exhumation of lower crustal material via solid-state advective flow implies that vertical crustal movements of at least part of the crust occurred independently of isostatic readjustments. *P–T* paths, characterized by isothermal decompression over a large pressure range, can therefore be interpreted to result from processes that are independent of crustal thickening, erosion and tectonic denudation.© 1997 Elsevier Science Ltd.

INTRODUCTION

Regional granulite terrains form a major component of shield areas in the world, and are of considerable interest because they may provide a window into the lower crust. However, it is not clear whether such granulite terrains represent typical lower crust as steady-state geotherm calculations suggest that granulites represent an anomalous situation (requiring very high heat flows of > 90 W/m^2; Chapman, 1986; Mezger, 1992). Regional granulite terrains probably develop in specific tectonic positions, e.g. along active orogenic zones and above mantle plumes. The tectonic processes and especially the crustal geometry and flow pattern involved in granulite formation and exhumation are not well known and form the subject of this paper.

To a large degree our understanding of tectonic processes in granulite belts is based on the interpretation of *P–T–t* paths (e.g. Harley, 1989) by comparing observed 'field paths' with computer-generated curves (England and Thompson, 1984; Chapman and Furlong, 1992). On the basis of *P–T* paths, two types of granulite terrains can be distinguished (e.g. Bohlen, 1987; Harley, 1989): those dominated by isobaric cooling (IBC) and those dominated by isothermal decompression (ITD). The ITD paths are generally related to crustal thickening and tectonic denudation (e.g. Harley, 1989; Anovitz and Chase, 1990). The IBC paths are thought to have resulted from either underplating of hot magma, tectonic interstacking of 'hot' and 'cold' crust (e.g. Spear *et al.*, 1990), or from the emplacement of large volumes of intrusive rock (e.g. Mezger, 1992).

It is questionable whether a good tectonic distinction can be made between granulite terrains based on the shape of the recorded *P–T* path alone. Problems with different retrograde re-equilibrations of geothermometers and geobarometers aside (e.g. Spear, 1993; Fitzsimons and Harley, 1994), *P–T* paths in many terrains may actually record several heating–cooling pulses superimposed on an overall decompressional path (Mezger, 1992; Dirks and Hand, 1995; Vernon, 1996). Apart from this (and perhaps due to this) a number of terrains record IBC and ITD paths side by side (e.g. Prydz Bay, Dirks and Hand, 1995; North Marginal Zone Limpopo Belt). This suggests that processes involved in the formation and exhumation of granulites may be more complicated (e.g. Audren and Triboulet, 1993; Dirks, 1995, 1996).

Textures and geometries in granulites mostly preserve evidence of their retrograde formation history. It is generally assumed that exhumation to surface occurred in response to isostatic re-equilibration, either during one, but more commonly during two or more, unrelated events (Ellis, 1987; Mezger, 1992). Where tectonic denudation is required to allow the rapid rise of granulites (core complexes, gneiss domes) and to explain observed ITD paths, low-angle extensional detachment zones are generally observed or inferred (Lister and Davies, 1989; Sandiford, 1989; Malavieille *et al.*, 1990; Kusky, 1993; Malavieille, 1993; Oliver, 1994; Zhang *et al.*, 1994). Especially when regionally persistent horizontal foliations occur, extensional collapse models have become very popular (e.g. Sandiford, 1989; Malavieille *et al.*, 1990; Zhang *et al.*, 1994). Such foliations are common in granulites, but unequivocal shear-sense indicators are not, and to assume that horizontal fabrics in granutites are related to extensional detachments is generally a large step. Several other mechanisms could lead to the development of such structures, including mechanisms that are unknown or absent in the upper crust, such as regional coaxial flow, repeated transposition and advective or convective flow (Dirks, 1996). In essence, little is known about the exact relationship between lower crustal geometries and observed *P–T* paths, or rather little is known about the mechanical behaviour of lower crustal material during granulite-facies metamorphism (Rutter and Brodie, 1991, 1992). In this paper we will describe the geometries that occur in a granulite terrain dominated by ITD, the Datong-Huai'an area, and try to interpret the tectonic regime that gave rise to the observed structures.

GEOLOGICAL SETTING

Granulites with Archaean ages ranging from 3800 to 2500 Ma (Liu *et al.*, 1996) are intermittently exposed along the northern margin of the North China Platform (Ma and Wu, 1981) (Fig. 1). Around Datong the granulites comprise a variety of pelitic, felsic and mafic units that were collectively grouped as the Jining Group (e.g. Shen *et al.*, 1989). This group was subdivided into a lower and an upper unit. The lower unit consists of a basement gneiss series (locally referred to as the TTG (trondjemite, tonalite, granodiorite) gneiss) that comprises a basal section dominated by mafic to intermediate granulites (gabbros, diorites tonalites and trondiemites), and a top section dominated by more felsic, biotite-rich enderbitic to charnockitic rocks, with scattered metapelitic horizons that serve as useful stratigraphic markers (Fig. 1). The upper unit consists of a metasedimentary cover sequence (locally called the Khondalite Series) that comprises Gnt–Sil-rich (mineral abbreviations after Kretz, 1983) metapelitic gneiss interbedded with garnetiferous felsic gneiss, granitic gneiss and, locally, lenses of mafic (two-pyroxene) gneiss (Condie *et al.*, 1992) intruded by numerous post-tectonic S-type granites.

Numerous dates, using a variety of isotope systems, have been reported from the Datong-Huai'an area (e.g. Shen *et al.*, 1987; Chen *et al.*, 1989; Zhai *et al.*, 1992; Guo, 1993). They confirm a complex multi-staged tectono-thermal history. Although incomplete data sets and a general lack of a comprehensive deformation scheme make it difficult to interpret many of the dates, a general picture does arise (Zhang *et al.*, 1994; Liu *et al.*, 1996). To summarize: an early crust-forming episode occurred during the mid-Archaean ($\sim$3500 Ma) and was followed by a further episode of crustal formation between 2700 and 2600 Ma. The metasedimentary cover rocks were probably deposited around this time. A first high-grade metamorphic event, associated with the formation of high-pressure granulites, most of the structural goeometries and numerous syn-tectonic charnockites, enderbites and tonalites, occurred between 2500 and 2400 Ma (Shen *et al.*, 1987; Guo, 1993). This event affected both the basement gneiss and metasedimentary cover units. A thermal event associated with granite intrusion may have occurred around 2200 Ma, although the exact nature of this event is unclear and ages recording this event may be mixing ages (Guo, 1993). Around 1900 Ma the area experienced a pervasive high-grade metamorphic overprint, visible as a second generation of granulite-grade assemblages and the intrusion of numerous granites. By 1800 Ma the area had stabilized and was exhumed to the surface as it is unconformably overlain by Mesoproterozoic sediments.

Granulites in Datong-Huai'an and surrounding areas, such as Zhangjiakou and Henshan (Fig. 1), characteristically preserve high-pressure assemblages in mafic units that formed between 2500 and 2400 Ma (e.g. Cui, 1982; Sills *et al.*, 1987; Shen *et al.*, 1989; Jin *et al.*, 1991; Wang *et al.*, 1991; Zhai *et al.*, 1992; Lu and Jin, 1993; Liu *et al.*, 1993; Zhang *et al.*, 1994). In felsic and pelitic units the high-pressure assemblages are largely destroyed and overprinted by lower *P–T* granulite-facies assemblages that resulted from several temporally unrelated events (e.g. Liu *et al.*, 1993; Zhang *et al.*, 1994). Various *P–T* estimates for the Datong-Huai'an area are presented in Table 1. In general, maximum pressure estimates from the basement gneisses originate from Grt–Qtz–Px-bearing mafic granulite lenses (Fig. 1) and record pressures between 12 and 16 kbar at temperatures between 800 and 900°C (e.g. Zhai *et al.*, 1992; Guo, 1993; Zhang *et al.*, 1994). Decompression coronas from these rocks yield estimates between 7 and 9 kbar and at 750–820°C (Liu,

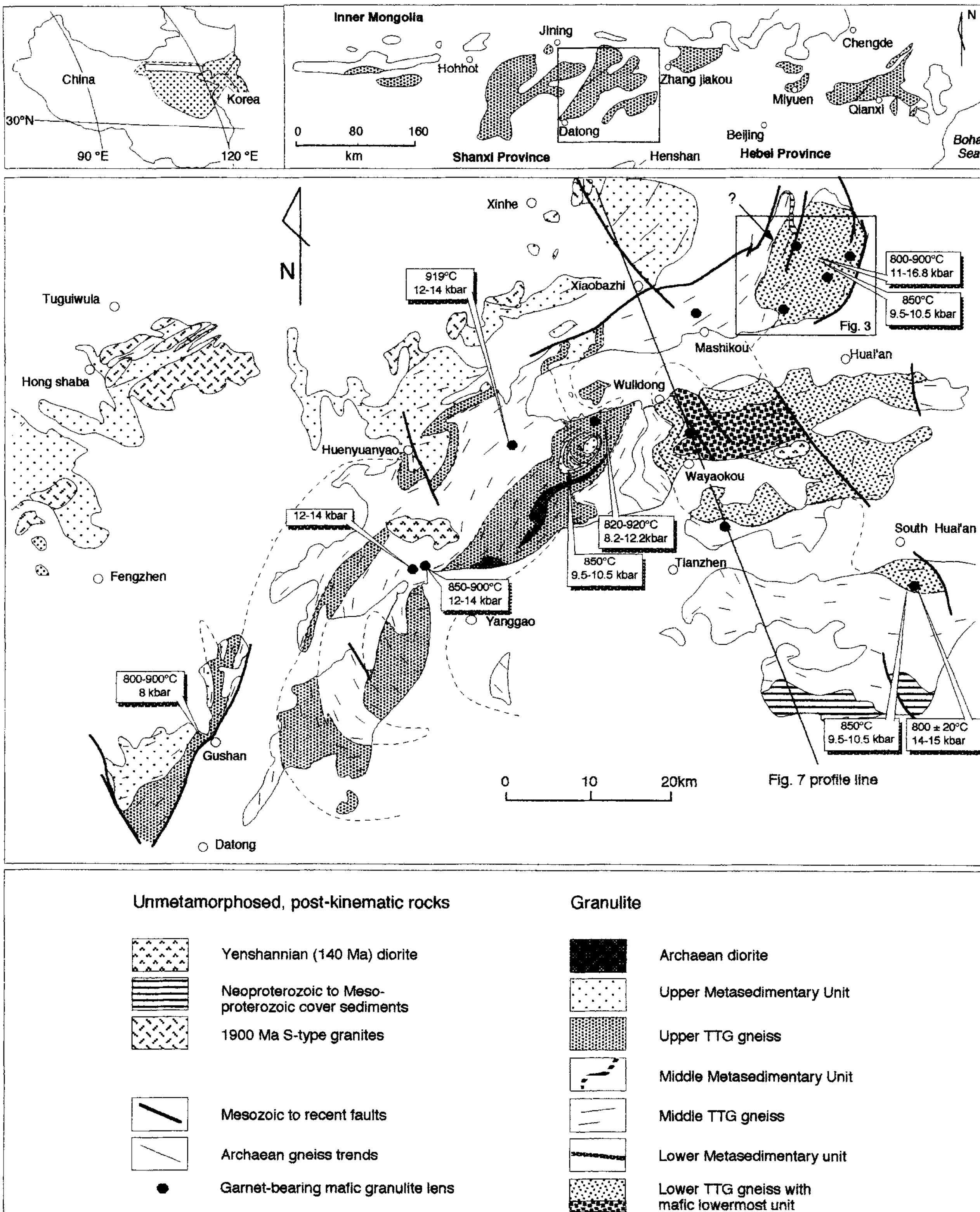

Fig. 1. Location and lithological map of Precambrian rocks (granulites plus cover) in the Datong-Huai'an area. The position of some of the garnet-bearing mafic granulite lenses that yield high metamorphic pressures is indicated.

1989; Zhai *et al.*, 1992; Zhang *et al.*, 1994) and formed during the dominant 2400–2500 Ma granulite event (Guo, 1993; Zhang *et al.*, 1994). Later reaction rims yield estimates of 4–6 kbar and 650–700°C (Zhang *et al.*, 1994) and formed as a result of thermal reactivation around 1900 Ma (Guo, 1993; Zhang *et al.*, 1994).

In metasedimentary rocks recorded peak assemblages range from 7 to 10 kbar at 700–900°C (Liu, 1989; Liu *et*

Table 1. Summary of published *P–T* results from the area around Datong (Fig. 1)

	Basement (= TTG) gneiss				Metasediments			
	Inclusion assemblage	Peak assemblage	Corona assemblage	Reaction rims	Inclusion assemblage	Peak assemblage	Corona assemblage	Reaction rims
	2500–2400 Ma			1900 Ma	2500–2400 Ma			1900 Ma
Liu (1989)		9–12 kbar, 880–940°C				8–10 kbar, 700–750°C	6.5–7 kbar, 700–750°C	
Zhai *et al.* (1992); Guo (1993)		14–15 kbar, 800±20°C	7–9 kbar, 820±20°C					
Lu and Jin (1993)					> 6–7 kbar, 600–700°C	8–10 kbar, 800±50°C		4–6 kbar, 700–750°C
Liu *et al.* (1993)		9.5±1 kbar, 845±20°C	9.5±1 kbar, 845±20°C			8±0.5 kbar, 690–750°C		4.1±0.5 kbar, 750–800°C
Zhang *et al.* (1994)	12–14 kbar, 800–900°C	10–14 kbar, 800–900°C	7–9 kbar, 750–800°C	4–6 kbar, 650–700°C		7–9 kbar, 800–900°C	7–9 kbar, 750–800°C	4–6 kbar, 650–700°C

al., 1993; Lu and Jin, 1993; Zhang *et al.*, 1994). A decompressional history of these rocks is suggested by the retrograde replacement of peak kyanite by sillimanite (Yan *et al.*, 1991; Lu and Jin, 1993) and the presence of plagioclase coronas on garnet in mafic lenses within the metasediments (Zhang *et al.*, 1994). Peak and corona assemblages formed during the main granulite event and affected the area at the end of the Archaean (Zhang *et al.*, 1994). Later reaction rims and high-grade shear zones were formed during a 1900 Ma metamorphic overprint (Zhang *et al.*, 1994), and yield *P–T* estimates of 4–6 kbar at 650–750°C (Liu *et al.*, 1993; Lu and Jin, 1993; Zhang *et al.*, 1994).

DEFORMATION GEOMETRIES IN HIGH-GRADE GRANULITE

Most of the geometries that are visible in outcrop in the Datong-Huia'an granulite terrain resulted from the events that occurred at the Archaean–Proterozoic boundary (Zhang *et al.*, 1994), which led to burial of metasediments and to the subsequent exhumation of deep crustal rocks from levels in excess of 50 km (15 kbar) to mid-crustal positions at about 20–25 km (7–8 kbar). Throughout the Datong-Huai'an area a tectono-stratigraphic sequence can be recognized. The term tectono-stratigraphy, as used here, refers to changes in rock type across a strongly deformed structural–metamorphic sequence dominated by a horizontal tectonic layering. It does not necessarily refer to original depositional divisions.

The tectono-stratigraphic sequence

In general, the granulites from Datong-Huai'an can be subdivided into six lithostratigraphic units (Fig. 1), which from old to young are: (1) the Lower TTG gneiss unit; (2) the Lower Metasediment unit; (3) the Middle TTG gneiss unit; (4) the Middle Metasediment unit; (5) the Upper TTG gneiss unit; and (6) the Upper Metasediment unit. All contacts between the metasedimentary and basement TTG gneiss units are tectonic (Wu *et al.*, 1994; Zhang *et al.*, 1994).

The Lower TTG gneiss unit is dominated by tonalite, enderbite, (quartz) diorite, and minor amounts of charnockite, meta-gabbro, pyroxenite and hornblendite. The main lithological units occur as sheets that parallel the gneissic layering. The thickness of such sheets varies from only a few centimetres, expressed as a felsic–mafic compositional layering, to kilometres in the case of large bodies of tonalite, granodiorite or charnockite. The mafic gneisses mainly occur in thin layers or isolated lenses that are up to 50 m wide, and may contain garnet. Opx- or Cpx-bearing anorthositic melt veins commonly occur in this unit, as do later granitic pegmatites. In general, the lower parts of the Lower TTG gneiss unit appear dominated by (> 50%) tonalites and mafic lithologies (diorites, gabbros), whilst structurally higher levels contain more (> 50%) trondhjemitic to charnockitic rocks (Fig. 1). Throughout the eastern part of the area, a laterally consistent Lower Metasediment unit separates the Lower and Middle TTG gneiss units (Fig. 1). The Lower Metasediment unit consists of Sil–Grt-rich metapelitic gneiss that is interbedded on a m- to dm-scale with Bt–Grt–Fs-rich metapsammitic gneiss and some matabasic gneiss. Around Wayaokou this unit occurs as a single 40–60 m thick layer, but northwest of Huai'an and south of South Huai'an the unit comprises several (three or more) 5–60 m thick layers that are interbedded or infolded with basement gneiss. The Middle TTG gneiss unit comprises the same rock types as the Lower TTG gneiss unit, but in different ratios. The Middle TTG gneiss is dominated by Bt-rich enderbitic and charnockitic units (> 50%), whilst diorites and tonalites are less abundant. A further characteristic is the presence of a large number of variably foliated Kfs-rich granitic gneisses (especially in the area southeast of Tianzhen,

Fig. 1). These intruded the charnockitic to dioritic gneiss units during the development of the main gneissic layering, and occur either as dm- to m-thick felsic sheets interbedded with the TTG gneiss, or as massive, probably sheet-like bodies. Overlying the Middle TTG gneiss unit occurs a laterally continuous, ~ 100 m wide, zone with numerous Grt–Bi–Fs–gneiss layers and lenses of ironstone, which have been grouped as the Middle Metasediment unit. The Upper TTG gneiss unit is similar to the Middle TTG gneiss unit, but overall it is more felsic (i.e. in the Yangao area, Fig. 1), and contains more pre-kinematic granitic and granodioritic units ($<30\%$), as well as more syn-kinematic Kfs-rich granites. The Upper TTG gneiss is topped by the Upper Metasediment unit. This unit is thick and, no doubt, structurally complex as it extends several hundreds of kilometres westward into Inner Mongolia. The Upper Metasediment unit consists of identical rocks to the Lower Metasediment unit. For a comprehensive description of the rock types see Condie *et al.* (1992).

STRUCTURE

In the Daton-Huai'an area evidence exists for three major high-grade structural events, overprinted by several episodes of later faulting. Early NW–SE-trending lineations associated with inclusion patterns of sillimanite in garnet may reflect prograde events and could be associated with the interleaving of basement gneiss and laterally continuous slivers of metasediment during an episode of burial and/or crustal thickening. The second, and by far the most prominent event in outcrop, is related to a pervasive shallowly SW-plunging lineation and exhumation of the high-pressure rocks. This exhumation process may be genetically linked to the first event via a process of crustal thickening and extensional collapse (Zhang *et al.*, 1994), but the exact processes involved are not clear. The third episode of deformation occurred later (1900 Ma) and was associated with discrete deformation zones in the Upper Metasediment unit and a static thermal overprint of the basement gneiss. Post-granulite grade deformation is restricted to Mesozoic (Yenshannian = 140 Ma) and Cenozoic block faulting and tilting, which partly reoriented the older structures. The amount of tilting, as estimated from non-metamorphosed and generally weakly deformed Meso- to Neoproterozoic (1840–900 Ma) and Jurassic–Cretaceous cover sequences, is generally less than 15°. Here we are mainly concerned with the second event that allowed the exhumation process to proceed.

Retrograde deformation: exhumation of high-pressure granulites

Most of the structures and all the tectonic foliations recognized in the area developed during the retrograde exhumation history of the high-pressure granulites (Zhang *et al.*, 1994; see below). On the basis of foliation–lineation patterns, two structural domains can be defined that developed at different structural/crustal levels and will be referred to here as the 'lower' and 'upper structural domain' (Fig. 2). Lineation patterns are the most useful discrimination tool between structural domains. Both domains are affected by multiple overprinting fold episodes that have fold axes parallel to the mineral and stretching lineation present in outcrop. These overprinting fold generations result in type 3 fold interference patterns and complicated foliation patterns. Structural trend maps in such terrains can be simplified if lineation (and colinear fold axes) directions are considered next to the foliation patterns (Dirks and Wilson, 1995). The lineation maps are more readily interpreted, e.g. refolding of the lineations is immediately obvious on a lineation map, but is not as clear on a corresponding foliation map that is already dominated by type 3 fold interference patterns.

Deformation sequences in the 'lower structural domain'

This domain comprises the rocks that occur near the base of the litho-stratigraphy. The contact with the 'upper structural domain' is more or less parallel to the base of the Lower Metasedimentary unit (Figs 1 & 2). It is characterized by: (1) highly variable foliation and lineation orientations, that are locally very steep; (2) the occurrence of more than one generation of gneissic layering, and hence truncation surfaces due to progressive transposition of different gneiss foliations; (3) the occurrence of numerous (at least six overprinting foliation-forming and folding events can be recognized in some outcrops) interfering fold episodes, many of which have parallel fold axes (colinear) in outcrop, even though fold axes orientations are highly variable in orientation on a regional scale; and (4) strong static recrystallization, which weakened the foliation and stretching lineations, and generally obliterated mineral lineations.

Structural characteristics of the 'lower structural domain' are best preserved in outcrops north of Huai'an (Fig. 2), where the gneiss has a coarse-grained granoblastic texture, and layering and lineations are strongly statically recrystallized. As a consequence, mineral lineations are limited to rare coarse-grained (>5 mm) Hbl-rich dioritic lenses or Opx-rich felsic gneiss. Elsewhere, lineations are stretching lineations that consist of mm- to cm-wide streaks or 'cigars' of felsic material in mafic gneiss, or vice versa. Coarsely banded felsic granulites generally do not contain a visible lineation.

North of Huai'an, the dominant gneissic layering defines domes with an approximate radius of 5–10 km (Figs 3 & 4b). As expected, foliations vary from near-horizontal in the centres of the dome to near-vertical along the margins. The domes comprise a broad antiformal central region that is bordered by a marginal zone with km-scale upright folds which appear to be more or less concentric around the dome (Fig. 3). The

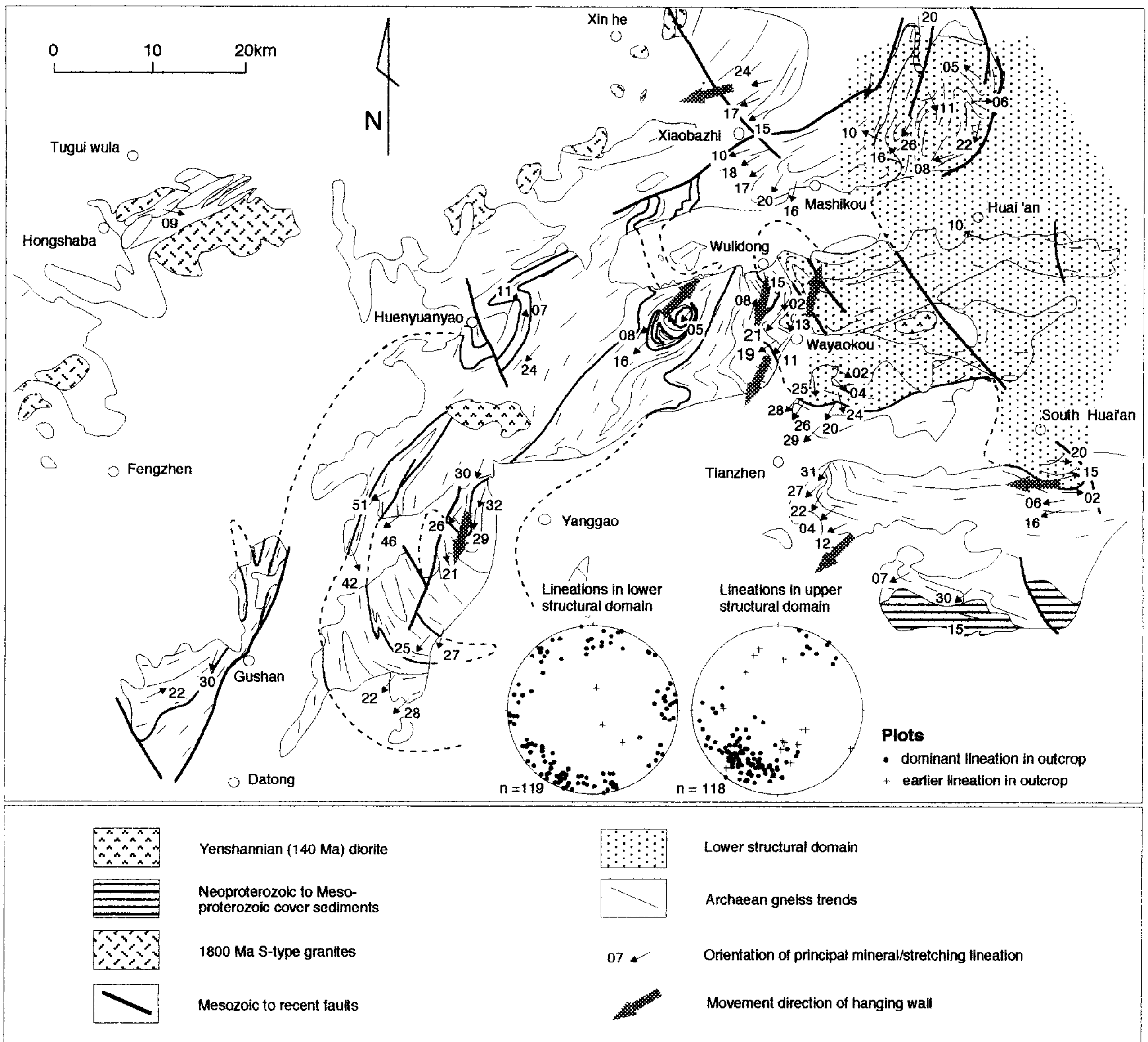

Fig. 2. The distribution pattern of the dominant lineation (mineral or stretching) in the Datong-Huai'an area. The position of the 'lower structural domain' is indicated. All other granulite-grade rocks constitute the 'upper structural domain'. The boundary between the Middle and Upper TTG gneiss units is indicated (bold black line).

lineations associated with the domed foliations plunge generally at less than 25° even where foliations steepen (Fig. 4). This means that the lineations do not define radial distribution patterns in which lineations plunge away from the centre of the culmination, as observed in mid-crustal gneiss domes and granite–greenstone terrains (e.g. Bateman, 1984; Jelsma *et al.*, 1993). Instead, lineation distribution patterns are concentric around the domes and occur within a more or less horizontal position along curving lines similar to the lines that represent great circles on a stereogram (Fig. 4).

Locally, where the gneissic layering is steep, more than one lineation is present. Here a generally steeply plunging lineation occurs next to a shallowly plunging lineation which is part of the regionally developed (or visible) lineation pattern. Both lineations are strongly recrystallized stretching lineations parallel to colinear crenulations and corrugations. The steeper lineations are commonly folded by open recumbent folds with fold axes that parallel the horizontal lineations. This observation, the regional continuity of the horizontal lineations and the only sporadical occurrence of the steeper lineation makes it likely that the steeper lineations are remnants of earlier transposed lineation patterns.

Not only lineation patterns are complicated, fold patterns are likewise extremely complex, although this is not immediately obvious in single outcrops (Fig. 3). In single outcrops (ignoring regional correlations and variations in orientation) a similar sequence of overprinting folds of different style can be observed everywhere. A typical sequence of overprinting fold styles is as follows (Fig. 5).

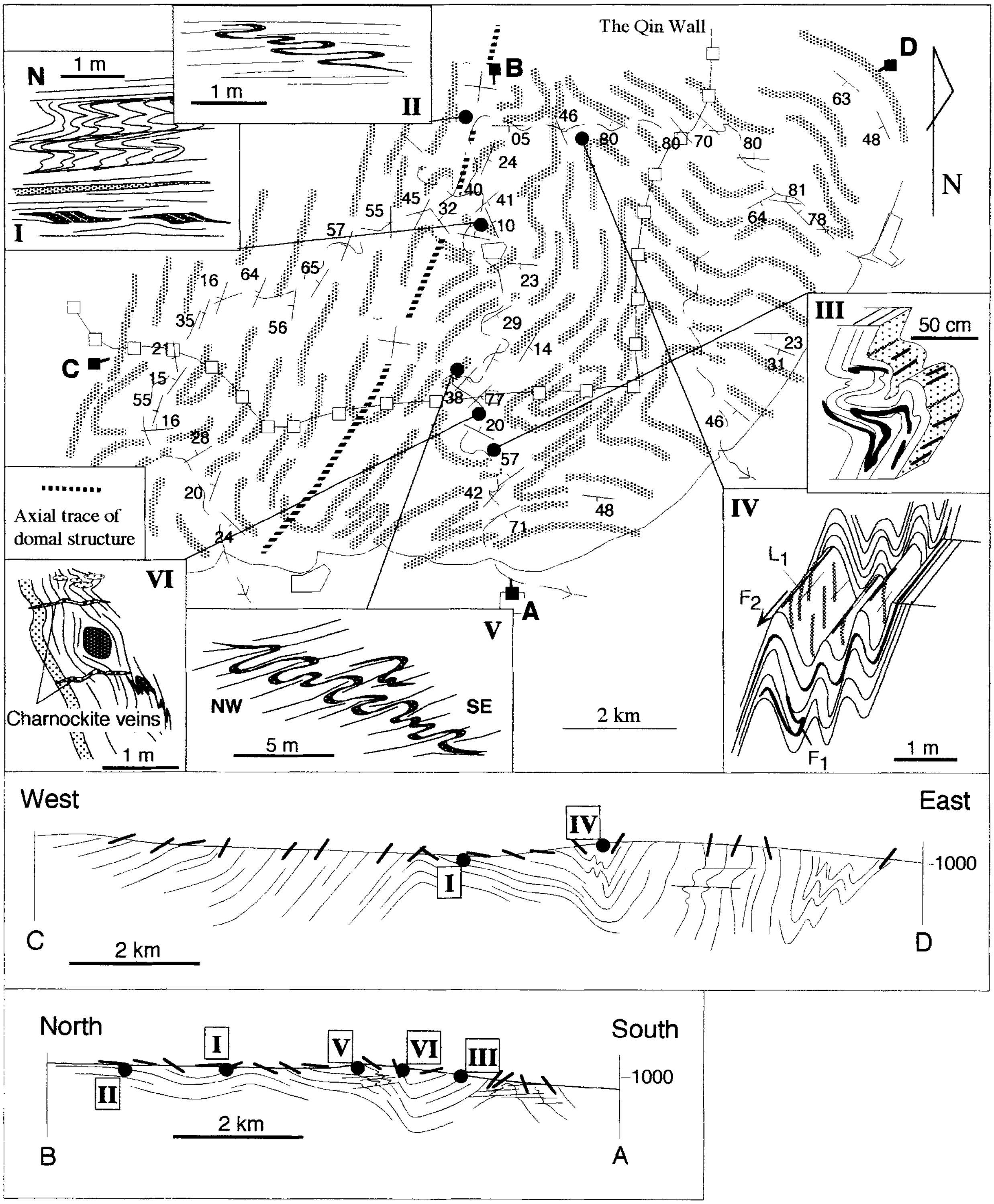

Fig. 3. Form surface map and cross-sections of typical domal fold geometries in the 'lower structural domain' north of Huai'an (see Fig. 2 for location). Insets show characteristic outcrop-scale fold/foliation patterns around the domes: near total transposition of tight recumbent folds occurs near and at the domal crests (I, II and V). Colinear upright and recumbent folds interfere in domal limbs (III and IV), while upright folds are most common in the synclinal zones between two domes (IV), where they locally fold an earlier lineation. Charnockitic melt veins are locally axial planar to the recumbent folds (VI).

Type 1—the earliest folds visible are isolated fold hinges and isoclinal intrafolial folds, usually defined by mafic layers in a more felsic matrix. It is not uncommon to find a clearly defined axial-planar gneissic layering defined by alternating Pl, Bt, Hbl or Px domains. If the compositional contrast between the folded layer and the matrix is small, these folds obtain a 'flame-like' smeared appearance. Fold axes to these folds parallel the stretching lineation (Fig. 5a).

Type 2—second generation folds consist of one or

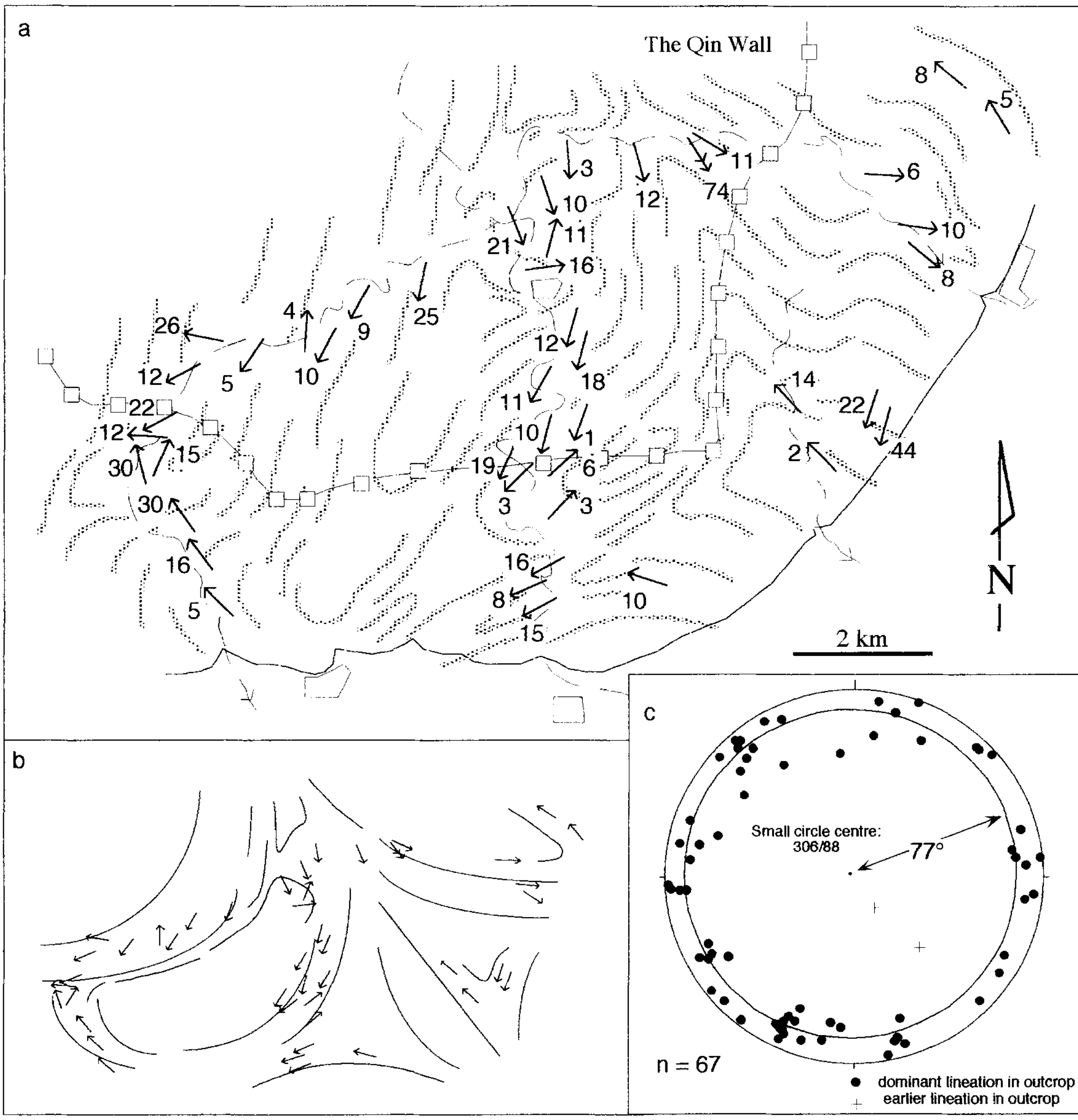

Fig. 4. (a) As Fig. 3, but shown is the distribution pattern of the dominant mineral and/or stretching lineation. (b) This lineation is mostly close to horizontal and shows a concentric variation around the (idealized) domes. (c) On a lower-hemisphere equal-area net the lineation directions show a small-circle distribution around a vertical axis with a conical angle of ~80°.

several generations of disharmonic open to isoclinal intrafolial folds, with weak axial-planar foliations and fold axes that parallel the stretching lineation. These folds may attain sheath-like geometries (Fig. 5b).

Type 3—open to closed recumbent folds, usually lacking an axial-planar foliation (except in the presence of Bt-rich lithologies), and fold axes that parallel the stretching lineation (Fig. 5c).

Type 4—late open to tight upright folds with weak or no axial-planar foliation and highly variable fold axes that do not parallel the stretching lineation (Fig. 5d).

Type 3 and 4 folds may also occur in reverse order. Apart from these, every outcrop is part of two types of regional-scale fold geometries (Fig. 5).

Type 5—changes in orientation of gneissic layering occurring on a 500–1000 m scale, whilst the orientation of the mineral elongation lineation remains unchanged. These folds include large-scale upright folds on either side of the dome.

Type 6—changes in both gneissic layering and the orientation of the mineral elongation lineation occurring on a 3–10 km scale to define the domal structures described above.

One consequence of this sequence of mostly colinear folds is that some outcrops viewed normal to the mineral elongation lineation, preserve complicated fold interference patterns. More commonly outcrops consist of a straight gneissic foliation with only a few type 1 and 2 fold hinges visible in outcrop. Correlations of folds from

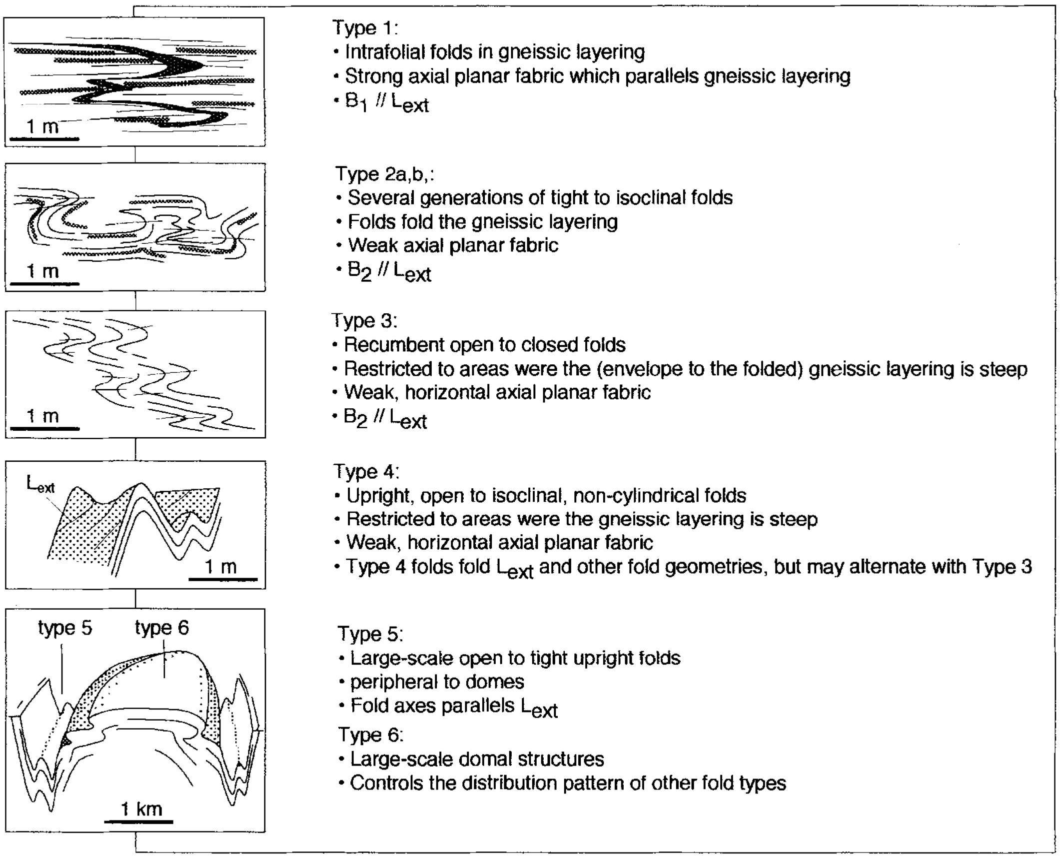

Fig. 5. The most important types of fold geometries encountered in the 'lower structural domain'. These fold geometries do not necessarily develop in sequence, although they do in outcrops where more complete fold histories are preserved. Type 5 and 6 folds constitute the large-scale fold geometries. Type 1 and 2 folds are common throughout the area, but constitute the sole fold type around the hinge region of type 6 domal folds. Type 3 folds are most common on the flanks of type 6 folds, where they overprint type 1 and 2 folds. Type 4 folds are most common as vergence structures in type 5 folds and may alternate with type 3 folds.

one outcrop to the next are hard to make. Instead it is more convenient to correlate groups of folds in outcrop 'A' to groups of folds in outcrop 'B'. Each of these fold groupings consist of all overprinting fold structures in an outcrop with fold axes directions that are identical and parallel to the mineral lineation. Comparisons of groups of folds are thus based on their identical relationship to this (regionally consistent) lineation direction, rather than relying on similarities in fold style.

To understand the development of type 1–4 fold geometries better, their distribution pattern in the larger-scale domal structures needs to be considered (Figs 3 & 6). In the near-horizontal culminations of the dome, only type 1 and 2 folds can be found, within a planar gneissic layering. Along the sides of the dome, the gneissic layering, including type 1 and 2 folds, steepen to near-vertical positions. Here, type 3 open to closed recumbent folds on a cm- to m-scale occur. Such recumbent folds vary in tightness; in places they are open corrugations that fold the dominant gneissic layering, elsewhere they are tight and consist of isolated fold hinge domains separated by domains with a new horizontal gneissic layering that is axial planar to the recumbent folds. Locally, the second flat-lying foliation becomes the dominant foliation in outcrop, in which the earlier foliation plus all its type 1–3 intrafolial folds are apparently completely transposed. The principle of this progressive transposition process is shown in Fig. 6. This new foliation is itself affected by further generations of type 3 recumbent folds. A characteristic of the marginal zones of the large-scale type 6 domes is the local dominance of numerous type 4 folds and the occurrence of remnants of an earlier second steep lineation. Type 4 folds either fold, or are folded by, type 3 recumbent folds, but domains exist, especially in synformal keels between two domes (Fig. 3), where type 4 folds are the sole geometrical feature. Type 5 and 6 folds define the large-scale geometries on which type 1–4 folds occur. The distribution pattern of fold types also suggests that type 1–3 folds represent different stages in a continuous transposition process, which started with a gneissic layering that was steepened along the sides of large-scale domes (Fig. 6). These steepened domains were progressively transposed in sets of recumbent folds to result ultimately in a new horizontal gneissic layering with type 1 folds (Fig. 6). The principal geometrical features in the

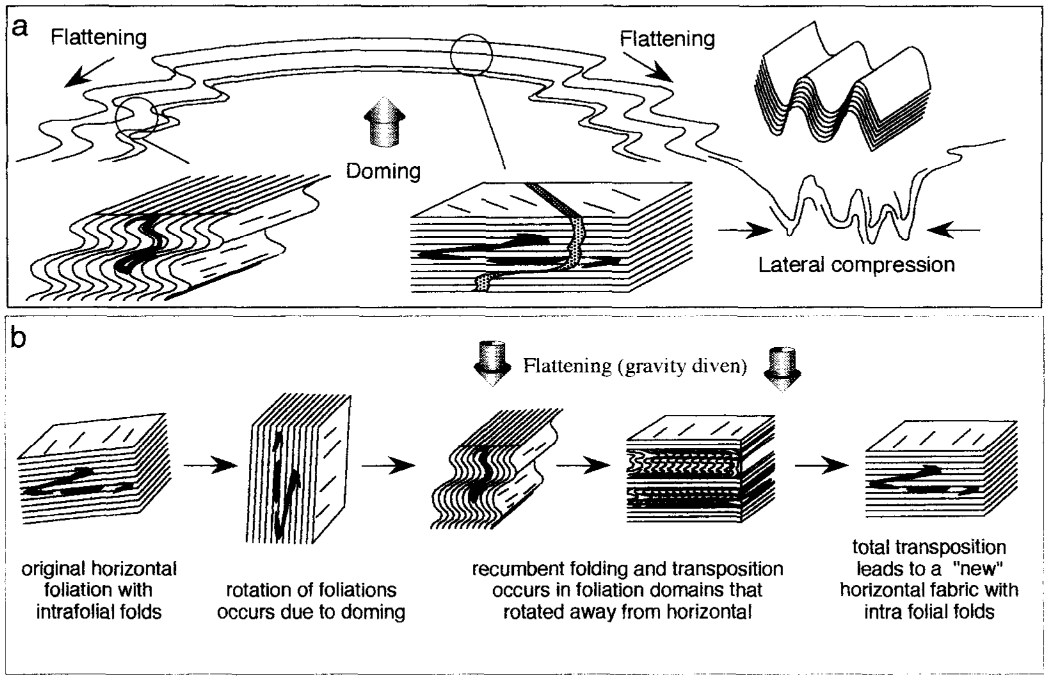

Fig. 6. (a) Idealized section through a domal fold and its peripheral synform (type 5 and 6 folds) as encountered in the 'lower structural domain'. The preferential occurrence of outcrop-scale fold geometries, such as intrafolial and recumbent folds (types 1–4 folds: Fig. 5), is indicated. (b) The gneissic foliation in the lower structural domain resulted from a process involving doming of an earlier horizontal layering followed by recumbent folding of the steepened limb regions of the domal structure. Progressive tightening of these recumbent folds ultimately leads to transposition of the earlier gneissic layering in a new gneissic layering with type 1 and 2 intrafolial folds (Fig. 5). This new layering may be domed again and the cycle repeats itself. As a result, any gneissic layering with several generations of type 1 and 2 intrafolial folds may have experienced several stages of transposition.

'lower structural domain' are, thus, domal structures separated by peripheral upright synforms, a radial lineation pattern within a horizontal plane and various stages of transposition leading to complicated fold and foliation interferences.

Deformation sequences in the 'upper structural domain'

This domain comprises most of the rocks that occur stratigraphically above the Lower TTG gneiss unit (Figs 1 & 2), and is characterized by: (1) a relatively constant lineation orientation plunging shallowly to the SW; (2) the occurrence of only one gneissic layering, with localized isoclinal intrafolial folds; (3) a few occurrences of interference folding on outcrop scale; and (4) clearly developed mineral lineations that are well preserved, probably because static recrystallization of the dominant fabric elements is not pervasive.

Although folding is less prominent in outcrop, fold sequences as described for the 'lower structural domain' occur in rocks belonging to the 'upper structural domain' as well. Type 1, 2 and 4 folds are the dominant fold types, type 3 open recumbent fold are rare and type 6 domal structures are not obvious, although slight variations in lineation orientation do occur and could be attributed to doming effects as described above (Fig. 2). The boundary between the 'lower' and 'upper structural domains' is not sharp, and domal structures from the lower domain do affect the upper domain.

Intrafolial folds in the 'upper structural domain' are locally seen on a km-scale. Ten kilometres southwest of Wulidong (Figs 1 & 2) lenses of the Upper Metasedimentary unit arc infolded with the basement gneiss to define flattened sheath folds with maximum diameters of the order of 2–3 km and fold axes that parallel the regional SW-plunging lineation (Wu *et al.*, 1994). The sheath folds are refolded on a km-scale in open to closed upright folds around a common lineation direction. These upright folds are the most dominant in the area and pervasive throughout the 'upper structural domain'. In a few locations, such as south of Xiaobazhl (Fig. 1), steep limbs of large-scale (type 4) upright folds preserve (type 3) recumbent folds (Fig. 7).

The planar foliations with constant near-horizontal lineation directions, as well as the colinear fold episodes, are characteristic of the 'upper structural domain' and probably resulted from shear (non-coaxial, constrictional flow) in a horizontal localization zone, which has been variably interpreted as an extensional shear (e.g. Zhang *et al.*, 1994) or a thrust (Wu *et al.*, 1994). To explain the decompression affecting the area, Zhang *et al.* (1994) suggested that the horizontal fabric formed in a low-angle detachment and was due to extensional collapse, with the top block moving to the southwest. In contrast,

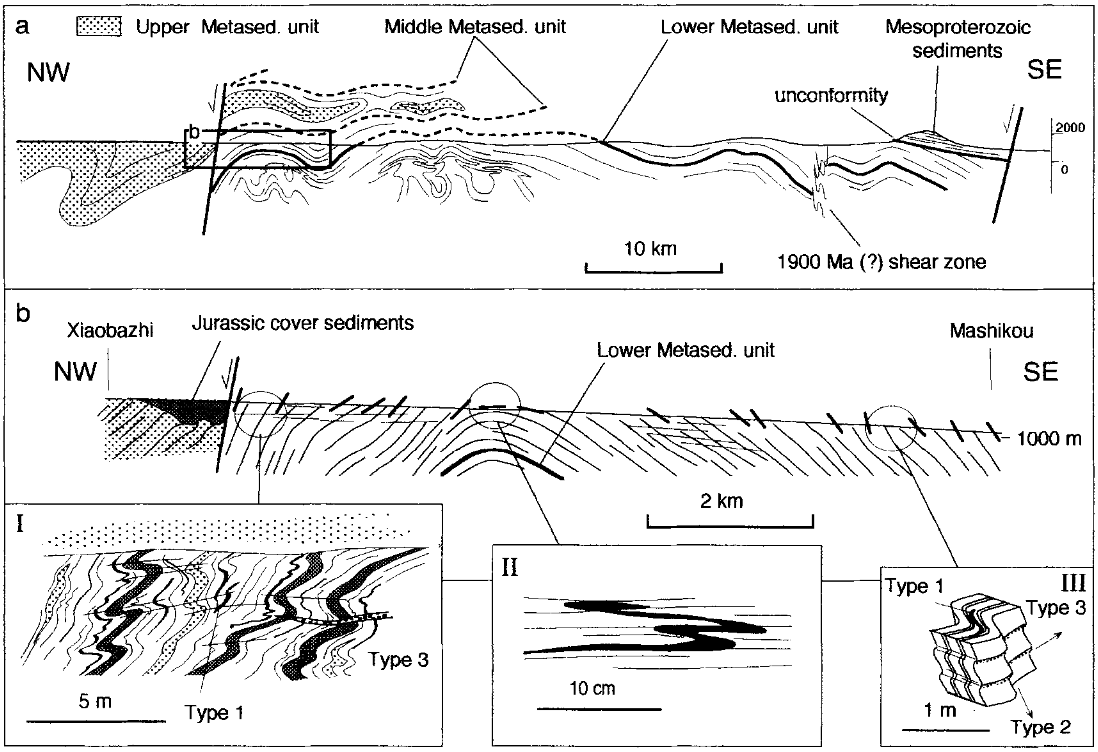

Fig. 7. (a) Structural cross-section showing the relationship between the 'lower structural domain' dominated by domal structures (domal geometries are exaggerated in this section) and the 'upper structural domain' dominated by an openly folded, planar fabric in which earlier sheath fold-like geometries are largely transposed. The position of the section line is given in Fig. 1. (b) Detail of the above section. This section occurs just above the transition zone between both domains and is presumably underlain by domal geometries as shown in Fig. 3 (schemetically shown as 'mushroom' structures in a). The upright folds in this part of the upper domain preserve recumbent folds along their limb regions (inset I and III) and intrafolial folds around the antiformal hinge region. In contrast to the 'lower structural domain', the apparent degree of transposition in new horizontal fabrics and scatter of lineation directions is limited.

Wu *et al.* (1994) concluded that the fabric with km-scale sheath folds formed due to NE-directed thrusting. An assessment of the attitude of flow is difficult as shear-sense indicators are rare and mostly of doubtful reliability as outlined below. In the 'upper structural domain' the following shear-sense indicators occur.

(1) Locally, Pl–Opx pseudomorphs after garnet are elongated in the extension lineation, and flattened to define a second foliation that makes a small angle with the dominant gneissic layering. The gneiss layering and flattened pseudomorph layering can be interpreted as *C* and *S* foliations, respectively. Where observed (e.g. west of Yangao) this texture is indicative of a top-to-the-south sense of shear.

(2) Large-scale, as well as small-scale, extensional shear bands with granitic vein fillings are common. In most places these seem to be associated with SW-directed displacement, but in a number of localities they indicate a top-to-the-NE shear sense. Both sets could be conjugates.

(3) Locally, felsic granulites contain isolated garnets and orthopyroxenes 1–5 cm in size. These have tails of retrograde biotite and hornblende that are asymmetric to define a geometry similar to that of delta-type mantled porphyroblasts (Passchier and Simpson, 1986). Delta clasts of this geometry would indicate a top-to-the-north sense of shear. Despite their resemblance to mantled delta-clasts, the porphyroblasts have a different internal structure and may have formed by a different mechanism (Passchier, 1994). It is therefore questionable as to whether they are reliable shear-sense indicators.

(4) All through the area asymmetric boudins occur. These generally consist of mafic lenses within a more felsic matrix and preserve an internal foliation that makes a slight angle with the external foliation, presumably due to rotation of the boudin (e.g. Hanmer and Passchier, 1991). In this way, both top-to-the-SW and top-to-the-NE displacements are indicated.

(5) Wu *et al.* (1994) defined a large-scale sheath fold 10 km southwest of Wulidong (Fig. 1) outlined by metapelites of the Upper Metasediment unit. The long axis of this structure plunges gently to the SW parallel to the mineral elongation lineation, and presumably the fold will close at depth. This geometry suggests an overall top-to-the-NE sense of shear.

All of the shear-sense indicators given above are difficult to interpret with certainty, and too few indicators occur to derive a general picture (Fig. 2). It appears that, in general, normal top-to-the-south or SW-directed flow is dominant, at least if the most commonly occurring shear bands and rotated boudins are considered. However, it is quite possible that the area represents mostly coaxial flattening, or a more complicated flow pattern in which NE- and SW-directed flow alternate.

The most pronounced fabric asymmetries do not occur in sections parallel to the lineations, but in sections normal to the foliation and lineation. Many recumbent folds that are colinear with the extension lineation are asymmetric when viewed normal to the fold axes. In general they verge away from antiformal hinge regions (Figs 6 & 7). This could be interpreted as flattening of the foliation in areas of domino, or upright, folding as transposition progresses (Figs 6 & 7). Isolated boudins commonly show rotations around the extensional lineation direction that are consistent with the asymmetries of the recumbent folds.

Relationships between structure and decompression textures in the structural domains

Peak metamorphic conditions as reported by Liu (1989), Zhai *et al.* (1992), and Zhang *et al.* (1994) were calculated from Grt-bearing mafic granulites. Some larger garnets in these rocks contain inclusions of Cpx–Pl–Qtz, which represent the assemblage that yields the highest *P–T* conditions (Zhang *et al.*, 1994). Such garnets are wrapped in the macroscopically visible gneissic foliation. Thus, peak metamorphic assemblages formed before the development of the gneissic foliations. The granoblastic matrix assemblages that define the principal foliation in the same gneisses yield pressures between 12 and 14 kbar (Table 1) indicating that the earliest gneissic foliations now visible in outcrop formed at high pressures.

Garnet in mafic, intermediate and felsic granulite is commonly replaced by coronas of Pl$\pm$Opx$\pm$Hbl$\pm$ Mag$\pm$Spl (Zhang *et al.*, 1994). In places these coronas are completely undeformed preserving delicate symplectic intergrowths unaffected by subsequent deformation. More commonly the replacement textures are recrystallized and locally elongated parallel to the stretching lineation or flattened in the axial planes of all fold types described above (Fig. 5). Depending on bulk composition, some general trends have been observed.

(1) Garnet pseudomorphs in two-pyroxene gneiss with subordinate amounts of Hbl–Qtz are mostly strongly recrystallized and deformed. Little garnet is preserved in these lithologies.

(2) Hbl-rich, two-pyroxene mafic rock with garnet and spinel, but no quartz, commonly contain significant amounts of garnet, that is generally only partly replaced by Pl–Opx–Hbl symplectites, which are mostly weakly deformed.

(3) Grt-bearing charnockitic to enderbitic units commonly preserve garnet with only narrow rims of plagioclase. These rims are locally extended along the mineral elongation lineation.

(4) In felsic units, garnets and their Pl–Opx coronas are commonly surrounded by a reaction rim of Hbl crystals and Bt, which are elongated in the mineral lineation.

The garnet replacement textures are all indicative of decompression cooling (Ringwood, 1975; Zhang *et al.*, 1994). Garnet stabilizes at lower pressures in silica-deficient mafic rocks (the Hbl-rich lithologies) and felsic rocks (like charnockites) compared to silica-saturated mafic rocks (Ringwood, 1975; Spear, 1993). Highly deformed and recrystallized replacement textures in silica-saturated mafic rocks yield *P–T* conditions as high as 12 kbar and 850–900°C, whereas little deformed replacement textures in charnockites or Hbl–Pl-rich lithologies yield pressures of 7–8 kbar at temperatures of $\sim$800°C (Zhai *et al.*, 1992; Zhang *et al.*, 1994) (Table 1). The former presumably formed earlier than the latter, but all formed during the progressive deformation that gave rise to the penetrative lineation. Thus, the geometries in the two structural domains described above were associated with exhumation from 14 to 7 kbar at elevated temperatures between 750 and 1000°C.

DISCUSSION

The salient features of the granulates at Datong-Huai'an are the occurrence of decompression textures in association with two structural domains that occur at different stratigraphic position, each characterized by specific foliation–lineation patterns (Figs 2–4). The vertically stratified, granulite-grade geometries potentially allow the formulation of a mechanism that accommodated exhumation of high-pressure granulites over vertical distances of 25–35 km. As both structural domains preserve identical assemblages and textures, and the contact between both domains is gradual, rocks may have passed from the 'lower' into the 'upper structural domain' during exhumation. To understand the dynamics of this process a careful interpretation of the geometries is required.

The 'lower structural domain' is defined as the stratigraphically lowest rocks and therefore represents the deepest portion of the 2400–2500 Ma crust. This crustal section is characterized by domes, highly variable horizontal lineation patterns, recumbent folds and transposition (Figs 3–5). The domal structures may be explained by comparing them with similar geometries that have been described in relation to regional interference folding magmatic and solid-state diapirism (mantled gneiss domes) or in the formation of extensional core complexes.

The structures in the 'lower structural domain' do not reflect a dome-and-basin fold interference pattern, because: (a) there appears to be no regular pattern in the occurrence of domes and basins; (b) there is no indication in the area that two independent folding events occurred with shortening directions at right angles; (c) no small-scale dome-and-basin-type fold interference structures occur in outcrop; and (d) 'vergence' folds along the limbs of the domes are recumbent and concentric around the domes.

The domal structures and surrounding concentric upright folds (Fig. 3) bear a resemblance to geometries associated with (ballooning) diapirs and mantled gneiss domes (e.g. Ramberg, 1981; Bateman, 1984; Van den Eeckhout *et al.*, 1986; Jackson and Talbot, 1989; Jelsma *et al.*, 1993). Also, the recumbent folds and horizontal fabrics can be equated with similar, although less intensely developed, features described around the flattened top of some gneiss domes (Van den Eeckhout *et al.*, 1986). When viewed in detail, however, idealized diapiric models differ from the domal structures in the Datong-Huai'an area because: (a) in the lower structural domain no intrusive diapirs or plutons occur in the centre of the domes and no (intrusive) margin or envelope to the domal structures can be defined. Instead lithologies in the centre of the domal structures are identical to those in the surrounding 'mantle' (this point is consistent with solid-state diapirs); (b) related to the above, strain intensities due to diapirism commonly increase towards the margin of a (diapiric) dome. Highest strains are expected along the contact of the diapir and its wall rock, which is characterized by a concentric (marginal), shear foliation. At Datong-Huai'an diapiric contacts cannot be identified and, as a result, concentric shear foliations and strain gradients towards the domal margins seem to be absent; and (c) the observed horizontal lineation patterns are significantly different to radial/tangential patterns predicted for model diapirs (Dixon and Summers, 1983; Jelsma *et al.*, 1993), even though some experimental results of complex diapirs do show similar concentric lineation patterns around domes (Ramberg, 1981).

Mantled gneiss domes or core complexes that rise from below a low-angle detachment and penetrate lower-grade rocks (Lister and Davies, 1989) also differ from the domes in the 'lower structural domain', which are not associated with an enveloping, marginal mylonite zone that accommodated unroofing, and allowed the rise of the domes in significantly lower-grade crust. Zhang *et al.* (1994) argued that the planar fabrics and the constant near-horizontal lineation of the 'upper structural domain' reflect the deep-crustal expression of a low-angle detachment zone. This model was put forward to explain the observed decompression textures in the basement gneisses, but is not unequivocally supported by the available shear-sense data. Besides, the 'upper structural domain' has a thickness of many kilometres and is not a discrete mylonite zone mantling the lower structural domain.

Vertical, solid-state diapiric or advective motion probably occurred to form the domal structures in the lower structural domain, but their geometries do not correspond to those described for typical (ballooning) diapirs, mantled gneiss domes or core complexes, which all involve clear lithological (viscosity) and metamorphic gradients between rising diapirs and their mantles (e.g. Dixon and Summers, 1983; Bateman, 1984; Lister and Davies, 1989; Audren and Triboulet, 1993). Most notable differences involve the lineation pattern and the extent and intensity at which recumbent folding and progressive transposition in horizontal foliations has taken place.

The presence of recumbent folds along the limb regions of the domes, the local progression of these recumbent folds in new transposition fabrics and the renewed doming of such transposition fabrics (e.g. south of Wulidong, Fig. 2) indicate that doming and flattening were dynamic and interacting processes during exhumation (Fig. 6). Domes may have developed from vertical and lateral expansion of a gneissic layering which originally had a constant lineation direction. Subsequent (or simultaneous) uniaxial flattening of such an expanding dome and transposition in new horizontal foliations would result in the more or less concentric stretching patterns reflected in the mineral lineations (Figs 4 & 6) (Dixon, 1975). Older lineations are readily recrystallized and eradicated during the process because of the very high metamorphic grades. The different truncating foliation domains with similar fold sequences, which can be observed in the lower structural domain, may reflect several 'frozen' stages of an alternating process involving doming–flattening–transposition–doming–flattening–transposition, etc. In this way, only the latest domes are preserved while much of the exhumation of high-pressure granulites actually took place via this doming–transposition mechanism.

Progressing from the 'lower' into the 'upper structural domain', the domal structures are gradually transposed within a planar gneissic layering with a relatively constant SW-plunging lineation direction (Fig. 7). The gneiss layering in the 'upper structural domain' is folded with fold axes parallel the mineral lineation, and a near-horizontal envelope. The presence of several sets of intrafolial folds and high-pressure assemblages with decompression textures suggests that vertical motion and transposition were important processes in the 'upper structural domain' as well, although flattening and lateral flow dominate the geometry. Large-scale, flattened, circular fold structures in this domain (Figs 1, 7 & 8) may represent sheath folds (Hanmer and Passchier, 1991; Wu *et al.*, 1994), but could also be cross-sections through portions of strongly flattened domal or basinal structures. Too few reliable shear-sense indicators occur to interpret confidently the kinematic attitude of the foliation in the upper structural domain. The colinearity of lineations and fold axes, and the overall fabric symmetry, suggests that horizontal flattening occurred in a constrictional environment. A top-to-the-SW normal sense of movement appears the most common (Fig. 2) and a degree of non-coaxiality could have occurred making it possible to equate the horizontal fabric with extensional flow (Sandiford, 1989; Zhang *et al.*, 1994), but such an interpretation is speculative.

During exhumation of the high-pressure granulites,

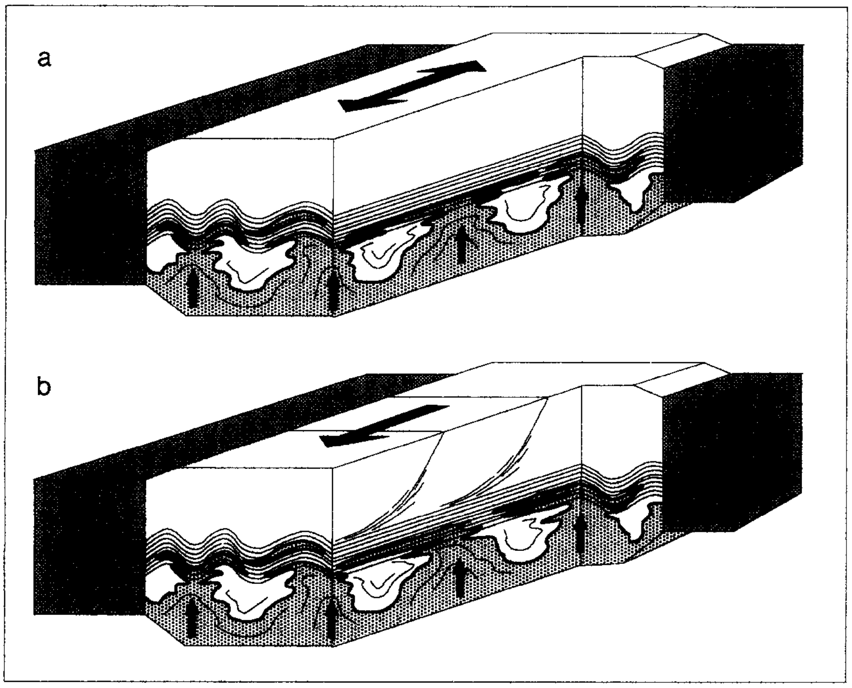

Fig. 8. Crustal model showing the possible larger scale positions of the 'lower' and 'upper structural domains'. The 'lower structural domain' is dominated by the solid-state diapiric rise of lower crustal granulite, which spreads sideways in the 'upper structural domain' as an inevitable consequence of transposition. This sideways flow may be largely coaxial (a) or non-coaxial (b), but either way it results in flattened, sheath-like fold geometries. Constrictional plate boundaries on either side of the granulite terrain may cause the uniform lineation distribution in the 'upper structural domain'. The lineation would parallel such boundaries, which can either be active (i.e. plates move inward) or passive (vertical flow of deep-crustal material in a restricted zone). For discussion, see text.

doming occurred simultaneously with transposition and flattening in a horizontal foliation. These processes dominated the finite strain fields at different crustal levels. If current outcrop patterns are representative, doming was the dominant process at crustal levels below ~30 km (9 kbar: calculated from weakly deformed coronas in the lower structural domain; Zhang *et al.*, 1994), whereas flattening and lateral flow dominated the strain field in the upper domain (Fig. 8). Owing to the intensity of flattening and horizontal transposition most domal structures have not preserved a domal outline, but have flattened to a pancake or surfboard-like shape. The lensoidal distribution pattern of lithological units may reflect this process (Fig. 8). Regional granulite terrains characterized by horizontal fabrics and decompression textures (e.g. Sandiford, 1989) may therefore 'hide' within the horizontal transposition fabric domal geometries reflecting vertical movements. The passage of rock from the 'lower structural domain' into the 'upper structural domain' can be explained in different ways. If vertical motion is considered as the overall dominant mechanism, the geometries may reflect a process of solid-state diapiric rise of material in the lower crust. This movement is arrested by a mechanical transition zone (a brittle–ductile transition) below which the diapirs spread out laterally in a mid-crustal zone dominated by coaxial flattening (Fig. 8a). Alternatively, horizontal crustal movements dominate and the 'upper structural domain' represents a mid-crustal zone characterized by non-coaxial deformation (e.g. a low-angle detachment zone) in which solid-state diapirs derived from lower levels can rise and become transposed (Fig. 8b).

The geometrical differences between domes described here and typical diapiric structures described for higher crustal levels (e.g. Brun and Pons, 1981) is probably a reflection of the rheology of the deep-crustal granulites. *In situ* rheological parameters for granulites in the presence of grain-boundary melt are largely unknown (e.g. Rutter and Brodie, 1991, 1992), but the viscosity of the rocks was probably sufficiently low to allow vertical movements driven by small variations in viscosity or density, possibly as a result of temperature gradients (Dirks, 1996). It raises the interesting question of whether convective flow is possible in such rocks.

The described, high-grade geometries of the Datong-Huai'an area carry some important metamorphic and tectonic implications. Exhumation of lower crustal material appears to have been accommodated, in part, by solid-state advective flow. Such flow would have been a very effective agent for heat transfer through the crust (Chapman, 1986; Mezger, 1992); a process enhanced by possible decompression melting (fluid absent bi-breakdown melting due to the near-adiabatic advective rise of lower crust) and granite emplacement to higher crustal levels (the volume of felsic material increases in the structurally higher domains). The thermal gradient associated with the granulites at Datong-Huia'an was therefore probably steep at shallow crustal levels, but very shallow at depth, and advective motion may have occurred through a large thickness of crust. Consequently, exhumation of parts of the crust occurred independently of isostatic processes (see also Audren and Triboulet, 1993).

If exhumation of deep crust is not necessarily the result of isostatic rebound, exposure of 16 kbar assemblages in the granulites at Datong-Huai'an did not automatically result from crustal thickening and the removal of 16 kbars of overburden ($\sim$50–55 km) by way of erosion or extensional collapse. It may be very wrong to assume that 55 km of overburden together with the present crustal thickness of $\sim$35 km presents a reliable minimum estimate of peak metamorphic crustal thicknesses during the 2500–2400 Ma collisional events. Such estimates of minimum crustal thickness during metamorphic peak conditions are commonly made in granulite terrains and are used in combination with decompression textures to explain clockwise *P–T* paths in terms of crustal thickening and extensional collapse.

Acknowledgements—This research project was supported by the foundation 'Stichting Schürmannfonds' (grant No. 94/10). J. S. Zhang received support from the National Science Foundation of China (grant No. 49070133) and the 'Department of Science and Education of The Netherlands' (grant HW/OI/UB 91053958 I). T. Blenkinsop is thanked for constructive critisisms which helped improve an earlier version of this manuscript. J.-C. Soula and G. Oliver are thanked for their constructive reviews.

REFERENCES

Anovitz, L. M. and Chase, C. G. (1990) Implications of post-thrusting extension and underplating for *P–T–t* paths in granulite terranes: a Grenville example. *Geology* **18**, 466–469.

Audren, C. and Triboulet, C. (1993) *P–T–t*-deformation paths recorded by kinzingites during diapirism in the western Variscan belt (Golfe du Morbihan, southern Brittany, France). *Journal of Metamorphic Geology* **11**, 337–356.

Bateman, R. (1984) On the role of diapirism in the segregation of ascent and final emplacement of granitoid magmas. *Tectonophysics* **11**, 211–231.

Bohlen, S. R. (1987) Pressure–temperature–time paths and a tectonic model for the evolution of granulites. *Journal of Geology* **95**, 617–632.

Brun, I. P. and Pons, J. (1981) Strain patterns of pluton emplacement in a crust undergoing non-coaxial deformation, Sierra Morena, southern Spain. *Journal of Structural Geology* **3**, 219–229.

Chapman, D. S. (1986) Thermal gradients in the continental crust. In *The Nature of the Lower Continental Crust*, eds J. B. Dawson, D. A. Carswell, J. Hall and K. H. Wedepohl, pp. 63–70. Geological Society of London Special Publication **24**.

Chapman, D. S. and Furlong, K. P. (1992) Thermal state of the continental lower crust. In *Continental Lower Crust*, eds. D. M. Fountain, R. Arculus and R. W. Kay, pp. 179–199. Elsevier, Amsterdam.

Chen, Y. P., Qian, X. and Liu, J. (1989) The sequence of the Archaean complex in the middle part of northern limit of the north China craton. In *Geological Sciences and Technology of the Lithosphere*, Vol. 2, pp. 53–60. Publishing House, Beijing University.

Condie, K. C., Boryta, M. D., Liu, J. Z. and Qian, X. L. (1992) The origin of khondalites: geochemical evidence from the Archean to Early Proterozoic granulite belt in the North China craton. *Precambrian Research* **59**, 207–223.

Cui, W. Y. (1982) The *P–T* condition of mineralogy and crystallography for granulites in the Zhuozi–Yanggao area. In *Collected Papers on Geological Research at Peking University*, pp. 110–121. Publishing House, Beijing University.

Dirks, P. H. G. M. (1995) Terrain interference in the Precambrian of Prydz Bay, east Antarctica. In *India and Antarctica During the Precambrian*, eds M. Yoshida and M. Santosh, pp. 177–202. Geological Society of India Memorial Volume **34**.

Dirks, P. H. G. M. (1996) On the importance of crustal convection in granulites. In *30th IGC, Beijing, China, Abstracts*, IGC p. 275.

Dirks, P. H. G. M. and Hand, M. (1995) Clarifying temperature–pressure paths via structures in granulite from the Bolingen Islands, Antarctica. *Australian Journal of Earth Sciences* **42**, 157–172.

Dirks, P. H. G. M. and Wilson, C. J. L. (1995) Crustal evolution of the East Antarctic mobile belt in Prydz Bay: continental collision at 500 Ma? *Precambrian Research* **75**, 189–207.

Dixon, J. M. (1975) Finite strain and progressive deformation in models of diapiric structures. *Tectonophysics* **28**, 89–124.

Dixon, J. M. and Summers, J. M. (1983) Patterns of total and incremental strain in subsiding troughs: experimental centrifuged models of inter-diapir synclines. *Canadian Journal of Earth Sciences* **20**, 1841–1861.

Ellis, D. J. (1987) Origin and evolution of granulites in normal and thickened crust. *Geology* **15**, 167–170.

England, P. C. and Thompson, A. B. (1984) Pressure–temperature–time paths of regional metamorphism. I. Heat transfer during the evolution of regions of thickened continental crust. *Journal of Petrology* **25**, 894–928.

Fitzsimons, I. C. W. and Harley, S. L. (1994) The influence of retrograde cation exchange on granulite *P–T* estimates and a convergence technique for the recovery of peak metamorphic conditions. *Journal of Petrology* **35**, 543–576.

Guo, J. H. (1993) The origin and evolution of the early Precambrian high pressure granulite melange belt and the granite belt, north China Craton. Ph.D. thesis, Academica Sinica, Beijing (in Chinese).

Hanmer, S. and Passchier, C.W. (1991) Shear-sense indicators: a review. *Geological Survey of Canada Paper* **90-17**, 1–72.

Harley, S. L. (1989) The origins of granulites: a metamorphic perspective. *Geological Magazine* **126**, 215–247.

Jackson, M. P. A. and Talbot, C. J. (1989) Anatomy of mushroom-shaped diapirs. *Journal of Structural Geology* **11**, 211–230.

Jelsma, H. A., van der Beck, P. A. and Vinyu, M. L. (1993) Tectonic evolution of the Bindura–Shamva Greenstone Belt (northern Zimbabwe): progressive deformation around diapiric structures. *Journal of Structural Geology* **15**, 163–176.

Jin, W., Li, S. and Liu, X. (1991) A study on characteristics of early Precambrian high-grade metamorphic rock series and their metamorphic dynamics. *Acta Petrologica Sinica* **4**, 2735.

Kretz, R. (1983) Symbols for rock forming minerals. *American Mineralogist* **68**, 277–279.

Kusky, T. M. (1993) Collapse of Archean orogens and the Generation of late- to postkinematic granitoids. *Geology* **21**, 925–928.

Lister, G. S. and Davies, G. A. (1989) The origin of metamorphic core complexes and detachment faults formed during Tertiary continental extension in the northern Colorado River region, U.S.A. *Journal of Structural Geology* **11**, 65–95.

Liu, D. Y., Geng, Y. S. and Song, B. (1996) Archaean crustal evolution in NW Hebei Province. In *30th IGC, Beijing, China, Abstracts*, IGC p. 526.

Liu, J. Z. (1989) Study of a lower crustal cross-section; Archaean cratonisation in central Inner Mongolia. Ph.D. thesis, Beijing University, Beijing (in Chinese).

Liu, X. S., Jin, W., Li, S. and Xu, X. C. (1993) Two types of Precambrian high-grade metamorphism, Inner Mongolia, China. *Journal of Metamorphic Geology* **11**, 499–510.

Lu, L.-Z. and Jin, S. Q. (1993) *P–T–t* paths and tectonic history of an early Precambrian granulite facies terrane, Jining District, south-east Inner Mongol, China. *Journal of Metamorphic Geology* **11**, 483–498.

Ma, X. Y. and Wu, Z. W. (1981) Early tectonic evolution of China. *Precambrian Research* **14**, 185–202.

Malavieille, J. (1993) Late orogenic extension in mountain belts: insights from the Basin and Range and the late Palcozoic Variscan belt. *Tectonics* **12**, 1115–1130.

Malavieille, J., Guihot, P., Costa, S., Lardeaux, J. M. and Gardien, V. (1990) Collapse of the thickened Variscan crust in the French Massif Central: Mont Pilat extensional shear zone and St. Etienne Late Carboniferous basin. *Tectonophysics* **177**, 139–149.

Mezger, K. (1992) Temporal evolution of regional granulite terrains:

implications for the formation of lowermost continental crust. In *Continental Lower Crust*, eds D. M. Fountain, R. Arculus and R. W. Kay, pp. 447–478. Elsevier, Amsterdam.

Oliver, G. J. H. (1994) Mid-crustal detachment and domes in the central zone of the Damaran orogen, Namibia. *Journal of African Earth Sciences* **19**, 331–344.

Passchier, C. W. (1994) Mixing in flow perturbations: a model for development of mantled porphyroclasts in mylonites. *Journal of Structural Geology* **16**, 733–736.

Passchier, C. W. and Simpson, C. (1986) Porphyroclast systems as kinematic indicators. *Journal of Structural Geology* **8**, 831–844.

Ramberg, H. (1981) *Gravity, Deformation and the Earth's Crust: Theory, Experiments and Geological Application.* Academic Press, London.

Ringwood, A. E. (1975) *Composition and Petrology of the Earth's Mantle.* McGraw-Hill, New York.

Rutter, E. H. and Brodie, K. H. (1991) Lithospheric rheology—a note of caution. *Journal of Structural Geology* **13**, 363–367.

Rutter, E. H. and Brodie, K. H. (1992) Rheology of the lower crust. In *Continental Lower Crust*, eds D. M. Fountain, R. Arculus and R. W. Kay, pp. 447–478. Elsevier, Amsterdam.

Sandiford, M. (1989) Horizontal structures in granulite terrains: a record of mountain building or mountain collapse? *Geology* **17**, 449–452.

Shen, Q. H., Liu, D. Y., Wang, P., Gao, J. and Zhang, Y. (1987) U–Pb and Rb–Sr isotopic age study of the Jining Group from Nei Mongol of China. (In Chinese.) *Bulletin of the Chinese Academy of Geological Sciences* **16**, 165–178.

Shen, Q. H., Zhang, Y., Gao, J. and Wang, P. (1989) The Archaean metamorphic rocks in mid-southern Inner Mongolia. *Bulletin of the Chinese Academy of Geological Sciences* **21**, 3–21.

Sills, J. D., Wang, K. Y., Yan, Y. and Windley, B. F. (1987) The Archaean high-grade gneiss terrain in E Hebei Province, NE China; geological framework and conditions of metamorphism. *Geological Society of London Special Publication* **27**, 297–305.

Soula, J.-C. (1982) Characteristics and mode of emplacement of gneiss domes and plutonic domes in central-eastern Pyrenees. *Journal of Structural Geology* **4**, 313–342.

Spear, F. S. (1993) *Metamorphic Phase Equilibria and Pressure–Temperature–Time Paths.* Mineralogical Society of America Monograph **1**.

Spear, F. S., Hickmott, D. D. and Selverstone, J. (1990) Metamorphic consequences of thrust emplacement, Fall Mountain, New Hampshire. *Bulletin of the Geological Societv of America* **102**, 1344–1360.

Van den Eeckhout, B., Grocott, J. and Vissers, R. (1986) On the role of diapirism in the segregation, ascent and final emplacement of granitoid magmas—Discussion. *Tectonophysics* **127**, 161–169.

Vernon, R.H. (1996) Problems with inferring *P–T–t* paths in low-*P* granulite facies rocks. *Journal of Metamorphic Geology* **14**.

Wang, R. M., Chen, Z. and Chen, F. (1991) Grey tonalitic gneiss and high-pressure granulite inclusions in Hengshan, Shanxi Province, and their geological significance. *Acta Petrologica Sinica* **4**, 36–45.

Wu, C. H., Gao, Y. D., Mei, H. L. and Zliong, C. T. (1994) Structural feature and unconformity arguments between khondalite suite and the granulite complex in Huangttiyao are, Nei Mongol, North China. In *Geological Evolution of the Granulites in the North Part of North China*, eds X. L. Qian and R. M. Wang. Seismological Publishing House, China.

Yan, Y. H., Zhai, M. and Guo, J. (1991) The cordierite–sillimanite assemblage ın the Archaean granulite belt on north China Platform as an indicator for low-pressure granulite facies. *Acta Petrologica Sinica* **4**, 46–56.

Zhai, M. G., Guo, J. H., Yan, Y. H., Han, X. L. and Li, Y. G. (1992) High pressure basic granulite and disclosing of a lowermost crust of the early Archaean continental type in N. *Institute of Geology, Academica Sinica, Advances in Geosciences* **2**, 126–139.

Zhang, J. S., Dirks, P. H. G. M. and Passchier, C. W. (1994) Extensional collapse and uplift in a polymetamorphic granulite terrain in the Archaean and Palaeoproterozoic of north China. *Precambrian Research* **67**, 37–57.